Cell, Vol. 109, 229–241, April 19, 2002, Copyright ©2002 by Cell Press

Spatial Representation of the Glomerular Map in the *Drosophila* Protocerebrum

Allan M. Wong,[1,3] Jing W. Wang,[1,3] and Richard Axel[1,2]

[1]Department of Biochemistry and Molecular Biophysics
Howard Hughes Medical Institute
College of Physicians and Surgeons
Columbia University
701 West 168th Street
New York, New York 10032

Summary

In the fruit fly, *Drosophila*, olfactory sensory neurons expressing a given receptor project to spatially invariant loci in the antennal lobe to create a topographic map of receptor activation. We have asked how the map in the antennal lobe is represented in higher sensory centers in the brain. Random labeling of individual projection neurons using the FLP-out technique reveals that projection neurons that innervate the same glomerulus exhibit strikingly similar axonal topography, whereas neurons from different glomeruli display very different patterns of projection in the protocerebrum. These results demonstrate that a topographic map of olfactory information is retained in higher brain centers, but the character of the map differs from that of the antennal lobe, affording an opportunity for integration of olfactory sensory input.

Introduction

Sensory neurons receive information from the environment and transmit this information to the brain where it is processed to create an internal representation of the external world. The representation of the sensory world in the brain then translates stimulus features into a neural code that discriminates complex sensory information and ultimately elicits a behavioral response. Most sensory systems spatially segregate afferent input from the peripheral sensory neurons to create a topographic map. In the auditory, somatosensory, and visual systems, neurons within the peripheral receptor sheet project to the central nervous system in a highly ordered manner, such that neighbor relations in the periphery are maintained in the brain. This orderly representation of cells in the peripheral receptor sheet may therefore transmit information to the brain concerning both the quality of a sensory stimulus and the position of a stimulus in space. The peripheral olfactory system does not extract spatial features of an odorant stimulus. Relieved of the requirement to map the position of an olfactory stimulus in space, the olfactory system may employ spatial segregation of sensory input to encode the quality of an odor.

We have examined how olfactory information is represented in the insect brain. Insects exhibit complex behaviors controlled by an olfactory sensory system that is significantly simpler than that of vertebrates. The recognition of odors in *Drosophila* is accomplished by sensory hairs distributed over the surface of the third antennal segment and the maxillary palp. Olfactory neurons within sensory hairs send projections to one of 43 glomeruli within the antennal lobe of the brain (Stocker, 1994; Laissue et al., 1999). The projection neurons (PNs) connect individual glomeruli with higher olfactory centers, the mushroom body, and protocerebrum (Stocker, 1994; Ito et al., 1998). Individual sensory neurons are likely to express only one of about 80 odorant receptor genes (Clyne et al., 1999; Gao and Chess, 1999; Vosshall et al., 2000; Scott et al., 2001; Dunipace et al., 2001; Stortkuhl and Kettler, 2001; Wetzel et al., 2001). In addition, about two-thirds of the neurons also express a common receptor gene, *Or83b*, such that neurons express a private and a public specificity (Vosshall et al., 2000). Neurons expressing the same receptors project with precision to one or rarely two spatially invariant glomeruli within the antennal lobe (Gao et al., 2000; Vosshall et al., 2000; Scott et al., 2001). A topographic map of receptor activity in the periphery is therefore represented in the antennal lobe. The segregation of like axons in the antennal lobe is in accord with 2-deoxyglucose mapping in the fruit fly (Rodrigues and Buchner, 1984; Rodrigues, 1988) and calcium imaging in the honeybee (Joerges et al., 1997; Galizia et al., 1999) that demonstrate that different odorants elicit defined patterns of glomerular activity.

The identification of a topographic map in which different odors elicit different patterns of activity in the antennal lobe has led to the suggestion that these spatial patterns reflect a code-defining odor quality (Vosshall et al., 2000; Gao et al., 2000). Others have argued, however, that the quality of an olfactory percept is encoded not in topography but in temporality, that different odors elicit different temporal patterns of activity and that this is a more relevant attribute of neural identity and odor quality than is position (Laurent, 1999). Whatever the code, patterns of activity in the antennal lobe must be translated by higher sensory centers to allow for the discrimination of complex olfactory information. Distinguishing among these models is likely to require an understanding of the neural circuit that translates odor recognition into specific behavioral responses. The circuit begins with primary olfactory neurons that project with precision to spatially invariant glomeruli. If odor quality is encoded by spatial patterns, we might expect that a representation of the glomerular map is retained in the protocerebrum.

We have therefore performed genetic experiments that permit us to visualize the projections of single PNs that connect defined glomeruli with their targets in the mushroom bodies and protocerebrum. We have used an enhancer trap line in which Gal4 is expressed in a subpopulation of projection neurons (Stocker et al., 1997), along with the FLP-out technique (Basler and Struhl, 1994) to label single projection neurons with a

[2]Correspondence: ra27@columbia.edu

[3]These authors contributed equally to this work.

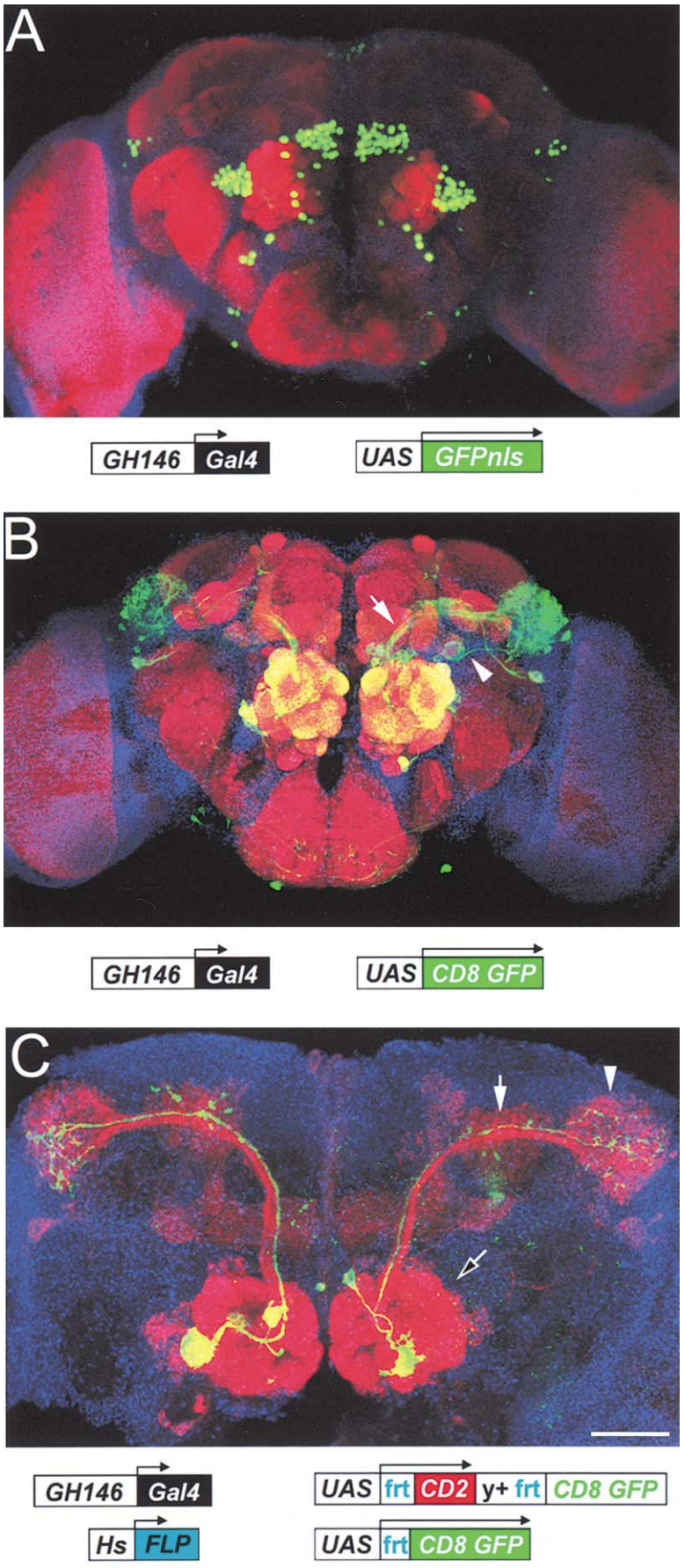

Figure 1. Visualizing the Projection Neurons Connecting the Antennal Lobe with the Protocerebum and Mushroom Body

(A) The enhancer trap line, *GH146-Gal4*, also bearing the transgene *UAS-GFPnls,* allows the visualization of PN nuclei surrounding the antennal lobe. Large clusters of dorsal and lateral nuclei, as well as a smaller cluster of ventral nuclei, are apparent. Staining is also consistently observed in small groups of cells surrounding the prototocerebrum as well as the subesophageal ganglion. In (A) and (B), brain whole- mount preparations were stained with anti-GFP (green), the monoclonal antibody, nc82, recognizing neuropil (red), and the nuclear stain TOTO-3 (blue). All preparations are fly brain whole mounts viewed frontally with dorsal on top.

(B) Flies bearing *GH146-Gal4* and *UAS-CD8-GFP* allow the visualization of the PN axons and dendrites. The PNs extend dendrites to glomeruli in the antennal lobe and axons to the mushroom body calyx and the lateral horn of the protocerebrum. A subset of PNs bypass the mushroom body and only innervate the protocerebrum. Arrow, inner antennocerebral tract (iACT); arrowhead, medial antennocerebral tract (mACT).

(C) *GH146-Gal4* flies carrying *UAS >CD2,y*$^{+}$*>CD8-GFP* and *Hs-flp* transgenes allow the visualization of the projections of single PNs. A mild heat shock was applied to third instar larvae to remove the *CD2* FLP-out cassette and place *CD8-GFP* under *UAS* control. Individual neurons with the *CD2* FLP-out cassette removed are visualized with anti-GFP (green), whereas the population of PNs that have an intact FLP-out cassette are visualized with anti-CD2 antibody (red). Open arrow, antennal lobe; filled arrow, mushroom body calyx; arrowhead, lateral horn of the protocerebrum. The scale bar equals 50 μm.

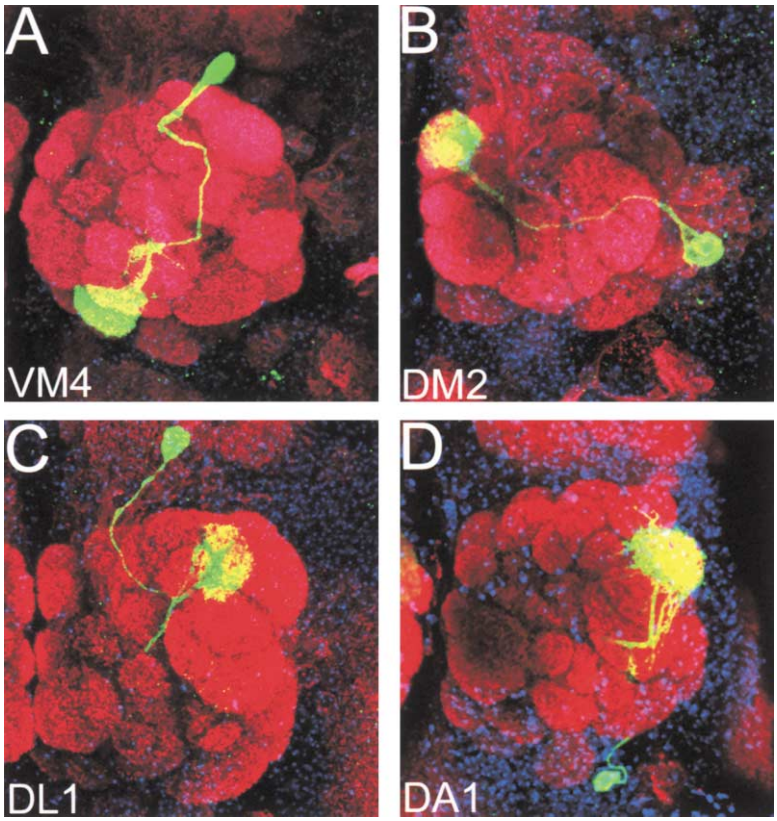

Figure 2. Visualizing the Dendritic Projections of Single PNs

GH146-Gal4 flies carrying the *Hs-flp* and *UAS >CD2,y+ >CD8-GFP* transgenes that have undergone FLP-out reveal that individual PNs project to a single glomerulus. Specific glomeruli were identified using the previously established antennal lobe map (Laissue et al., 1999). No apparent spatial relationship between the position of the cell body and the glomerulus can be discerned, but the cell group in which cell bodies reside are maintained in all flies examined. (A) VM4, (B) DM2, (C) DL1, and (D) DA1.

CD8-GFP reporter. A similar experimental approach has recently been used to determine the lineage relationship of individual PNs (Jefferis et al., 2001) and in a companion study to examine their pattern of axonal projections (Marin et al., 2002 [this issue of *Cell*]). We observe that most PNs send dendrites to a single glomerulus. Projection neurons that receive input from a given glomerulus extend axons that form a spatially invariant pattern in the protocerebrum. PNs from different glomeruli exhibit patterns of axonal projections that are distinct but often interdigitate. These results demonstrate that a topographic map of olfactory information is retained in higher brain centers, but the character of the map differs from that of the antennal lobe. The tight segregation of individual sensory axons observed in the antennal lobe is replaced by an overlapping but stereotyped distribution of axonal arbors in the protocerebrum, affording the opportunity for integration of input from multiple glomeruli.

Results

Visualizing a Subpopulation of Projection Neurons

Genetic experiments with the *Drosophila* odorant receptor genes have allowed the visualization of a topographic map of sensory projections in the antennal lobe (Gao et al., 2000; Vosshall et al., 2000; Scott et al., 2001). We now ask whether the representation of receptor activation in the antennal lobe is maintained by the projection neurons that connect glomeruli to higher order olfactory centers. Anatomic studies identify about 200 projection neurons (Stocker et al., 1990). PN cell bodies surround the antennal lobe and the dendrites of most PNs innervate a single glomerulus. The PN axons project through one of three ascending tracts, the inner antennocerebral tract (iACT) that projects to the calyx of the mushroom body and protocerebrum and the medial (mACT) and outer (oACT) antennocerebral tracts that bypass the mushroom body and innervate the protocerebrum.

An enhancer trap line, *GH146-Gal4*, has been characterized that drives the expression of *Gal4* in 83 of the PNs, allowing visualization of a large subpopulation of projection neurons (Stocker et al., 1997; Jefferis et al., 2001). In initial experiments, we crossed the *GH146-Gal4* line to flies bearing a *UAS-GFPnls* transgene that encodes a GFP molecule bearing a nuclear localization signal. We observe GFP expression in the nuclei of 83 (83 ± 2, $n = 6$) PNs surrounding the antennal lobe (Figure 1A). The cell bodies of GH146-positive PNs expressing *Gal4* reside in three anatomically discrete groups circumscribing the antennal lobe with 41 (41 ± 3, $n = 6$) dorsal-anterior, 34 (34 ± 2, $n = 6$) lateral, and 7 (7 ± 3, $n = 6$) ventral PNs. In addition, GFP is also observed in six cells posterior and lateral to the protocerebrum and three cells ventral to the subesophageal ganglia that are not projection neurons.

The projections of the population of 83 PNs can be visualized in a cross between the *GH146-Gal4* line and flies bearing the transgene *UAS-CD8-GFP*, which encodes a membrane-tethered GFP decorating both axonal and dendritic projections (Figure 1B). In these flies, robust glomerular staining is observed in 34 anatomically defined glomeruli in the antennal lobe. The majority of the projection neurons expressing CD8-GFP send

axons through the iACT and synapse both in the calyx of the mushroom body and the lateral protocerebrum. *Gal4* is also expressed in at least four neurons that send processes through the mACT and a single neuron that projects axons via the oACT. These two fiber tracts bypass the mushroom body and connect glomeruli directly to the protocerebrum (see below; Stocker et al., 1997; Ito et al., 1998).

Visualizing the Projections of Individual PNs in the Antennal Lobe

We next examined the projections of individual PNs that connect specific glomeruli to their protocerebral targets. Genetic markers that define individual PNs have not been identified. We therefore employed the *GH146-Gal4* enhancer-trap line, in concert with the FLP-out technique, to express a transmembrane reporter CD8-GFP in single-projection neurons (Nellen et al., 1996; Zecca et al., 1996). In order to obtain single cells expressing CD8-GFP, we generated larvae from *GH146-Gal4* lines that also carry the transgenes *UAS >CD2,y$^+$>CD8-GFP* and *Hs-flp*. Excision of the *CD2,y$^+$* FLP-out cassette is mediated by a mild heat shock during late third instar, a stage when projection neurons are postmitotic and specified (Jefferis et al., 2001). Excision of the FLP-out cassette in random subpopulations of PNs, and at the extreme, in single PNs, can be visualized by CD8-GFP expression. In flies treated in this manner, CD2 is expressed in the cell bodies and processes of a large population of PNs and identifies the projections to the mushroom body and the protocerebrum. The expression of CD8-GFP allows the visualization of the dendritic and axonal arbors of only a single-projection neuron (Figure 1C). Since most individual glomeruli within the antennal lobe are morphologically distinct and spatially invariant, it is possible to identify the individual PNs that connect to a defined glomerulus and trace its axonal projections from the antennal lobe to the mushroom body and the protocerebrum. Examination of over 2,000 fly brains has allowed us to trace the pattern of projections of 147 individual PNs from their dendritic glomerular arbor to their axonal target.

Analysis of the dendritic projections of 147 individual PNs within the glomerulus of the antennal lobe reveals several features of a dendritic map (Figure 2 and Table 1). First, individual projection neurons extend dendrites to only a single glomerulus (Figure 2), a finding in accord with previous studies using Golgi staining (Stocker et al., 1990) as well as more recent genetic tracing experiments (Jefferis et al., 2001). Second, the cell bodies of PNs whose dendrites occupy a given glomerulus usually reside within only one of the three cell groups. For example, the PNs that receive input from the DM2 glomerulus reside within the lateral cell grouping, whereas the neurons with dendrites in the VM4 and DL1 glomerulus reside within the dorsal-anterior population of PNs (Figure 2). The location of the cell bodies of specific PNs is maintained from organism to organism. Finally, no neighbor relationship is observed for the location of the PN cell body and the glomerulus, which it innervates. The PNs of DA1, VM4, and DM2, for example, are distant from their glomeruli, whereas the DL1 PN is adjacent to its glomerulus (Figure 2). Although most glomeruli connect to cell bodies within only one of the three groups of PNs, two glomeruli (VA1lm and DA1) connect with PNs whose cell bodies reside within two groups (see below).

Table 1. Distribution of Single Projection Neurons

Glomerulus	Soma position	Number of samples
D	Dorsal	4
DA1	Lateral	3
	Ventral	3
DA2	Lateral	4
DA3	Dorsal	3
DC1	Dorsal	2
DC3	Dorsal	3
DL1	Dorsal	9
DL4	Dorsal	4
DM1	Lateral	2
DM2	Lateral	8
DM4	Dorsal	2
DM5	Lateral	1
DM6	Dorsal	3
DP1m	Dorsal	2
VA1d	Dorsal	7
VA1lm	Dorsal	12
	Ventral	5
VA2	Dorsal	4
VA2p	Lateral	2
VA3	Dorsal	3
VA4	Lateral	5
VA5	Lateral	6
VA6	Dorsal	6
VA7lm	Lateral	6
VC1	Lateral	2
VC2	Lateral	1
VL2a	Dorsal	7
VL2p	Dorsal	3
VM1	Lateral	3
VM2	Dorsal	10
VM3	Dorsal	3
VM4	Dorsal	2
VM7	Dorsal	3
1	Dorsal	3
asterisk	Dorsal	1
Total		147

Projections of Individual PNs in the Protocerebrum

We next asked how the topographic map in the antennal lobe is represented in higher olfactory centers in the fly brain. We therefore analyzed the patterns of axonal projections of 147 individual PNs in the mushroom body and protocerebrum (Figures 3 and 4; Table 1). In *GH146-Gal4* flies, *Gal4* is expressed in 83 PNs that innervate 34 glomeruli, implying that on average each glomerulus receives dendrites from three PNs. It is therefore possible to examine the axonal patterns from multiple, different PNs that innervate the same glomerulus. For example, we have visualized the pattern of axonal projections of four independent PNs that connect the DA2 glomerulus to the protocerebrum (Figure 3A). The cell bodies of the DA2 PNs reside within the lateral group of neurons and project axons through the iACT. DA2 axons send a single branch to the calyx of the mushroom body and extend into the protocerebrum. The DA2 axon then splits into two branches that arborize in the medial portion of

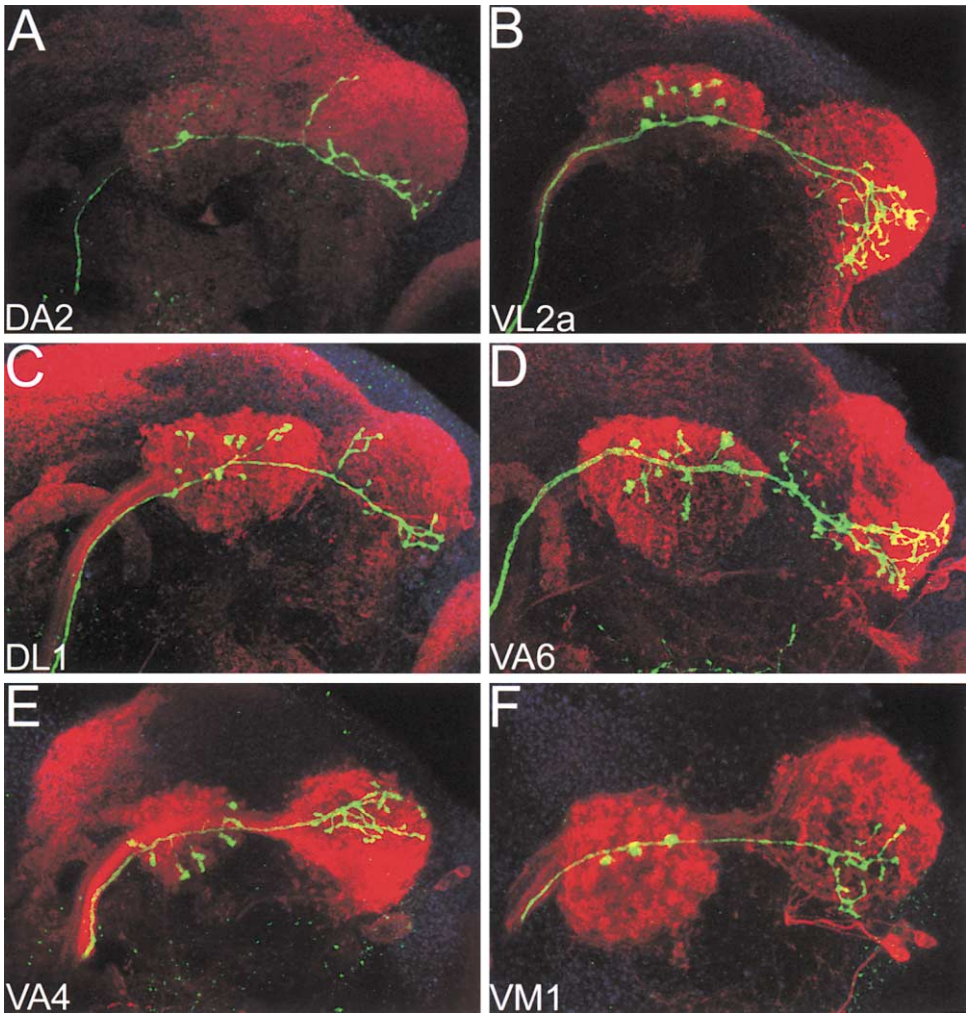

Figure 3. Axonal Projections from PNs that Connect to Different Glomeruli Are Distinct

The axonal projections from single PNs can be visualized as they course through the antennal cerebral tract, branch in the mushroom body, and ultimately arborize in the lateral horn of the protocerebrum. PNs that connect to different glomeruli exhibit different patterns of axonal projections that are reflected both in the branching pattern in the mushroom body and the branching and arborization in the protocerebrum. The generation of single-labeled PNs and the staining was performed as described in for Figure 2.

the lateral protocerebrum. The pattern of branching and the arborization is strikingly similar for each of the four DA2 PNs visualized (Figure 6B). In contrast, the cell bodies of PNs that innervate the VL2a glomerulus reside solely within the dorsal cell group (Figure 3B). Axons from the seven individual VL2a PNs exhibit a characteristic pattern of branching and arborization, distinct from DA2 axons, in a more lateral domain of the protocerebrum (Figures 3C and 6B). Even when projection patterns appear to overlap in two dimensions, as is the case for VM1 (Figure 3F) and VA1lm (Figures 5C and 5D), the axonal arbors are distinct when examined in three dimensions, with VM1 branching more posteriorly than VA1lm in the ventral protocerebrum.

Analysis of the projections of 147 PNs that innervate 34 glomeruli reveals that PNs that receive input from different glomeruli exhibit different spatial patterns of axonal arborization (Figure 3). However, projection neurons that innervate the same glomerulus reveal strikingly similar projection patterns, and this pattern is conserved in different organisms (Figure 4). For example, we have analyzed projection profiles of five ventral VA1lm PNs (Figures 4A–4D) and observe a strong concordance in the patterns of axon branching and arborization. This stereotypic invariance of axonal arbors is apparent for all PNs for which we have multiple examples (Figures 4 and 6B; Table 1). Although PNs innervating a given glomerulus exhibit invariant projections, the topographic order of glomeruli in the antennal lobe is not maintained in the protocerebrum. Thus, PNs innervating neighboring glomeruli reveal projections that can be distant from one another in the protocerebrum.

On average, each glomerulus receives dendrites from three labeled projection neurons. If the heat shock FLP-out technique randomly labels PNs with equal frequency, our data would imply that all neurons that connect to a given glomerulus reveal similar projection patterns. Alternatively, the FLP-out labeling approach may be nonrandom, such that one of the multiple projection neurons from a single glomerulus may be more suscepti-

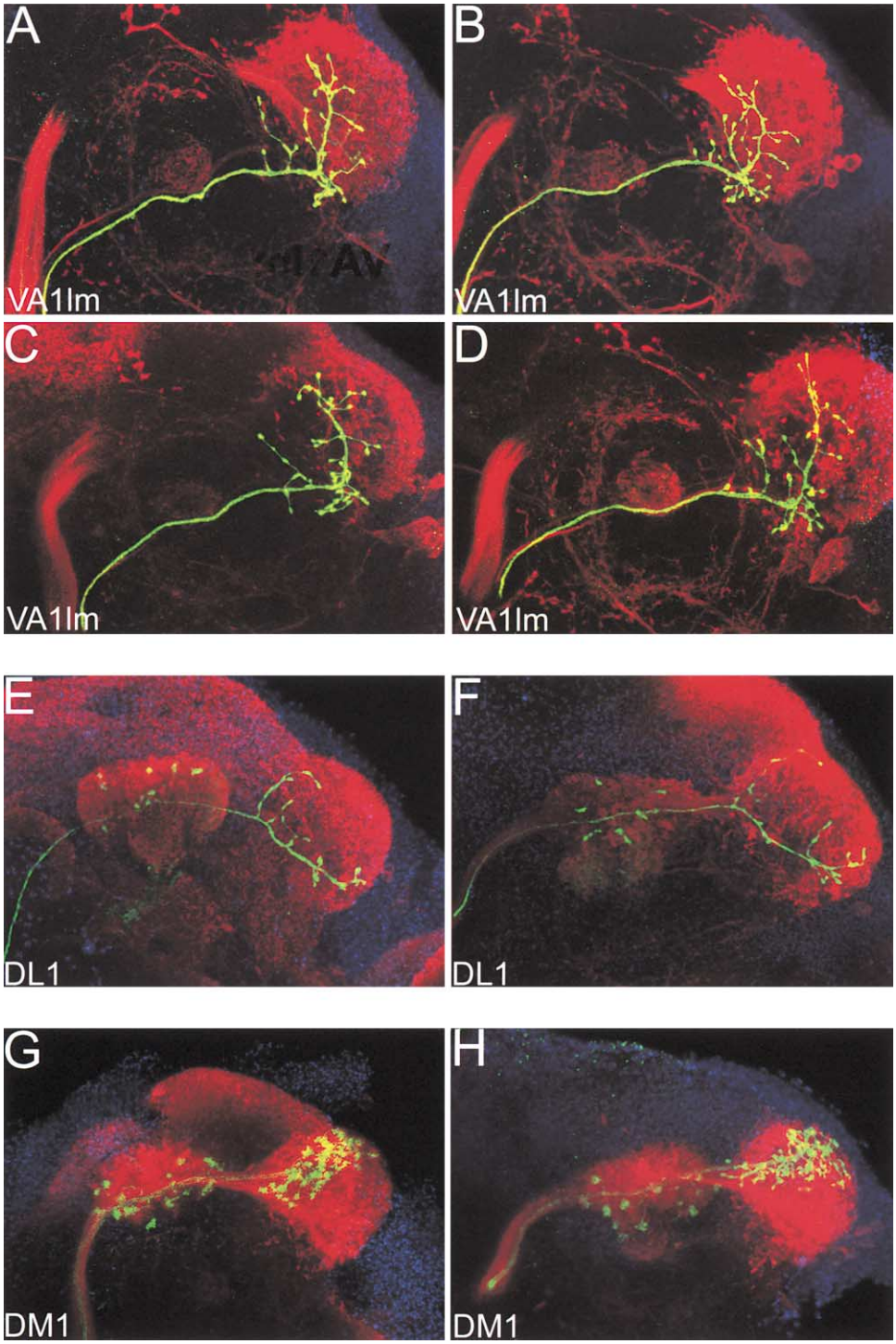

Figure 4. Projection Neurons that Connect to the Same Glomerulus Have Similar Axonal Projection Patterns

Individual projection neurons that connect to the VA1lm (A–D), DL1 (E and F), and DM1 (G and H) glomeruli were followed into the mushroom body and protocerebrum in different flies. Representative images are shown and reveal that PNs that project to different glomeruli display different axonal pattern (Figure 3), whereas a striking constancy in projection pattern is observed among PNs that project to a given glomerulus.

ble to FLP-out. If true, each of the three PNs connected to a given glomerulus might reveal distinct arborization patterns, but this would not be detected in our analysis. In order to distinguish among these alternatives, we have searched brain preparations that contain two labeled projection neurons that connect to the same glomerulus. Although rare, we have obtained brain samples with two PNs innervating VA7ml or VA5 (data not shown). In each instance, the cell bodies of neurons that connect to a given glomerulus reside within the same cell group

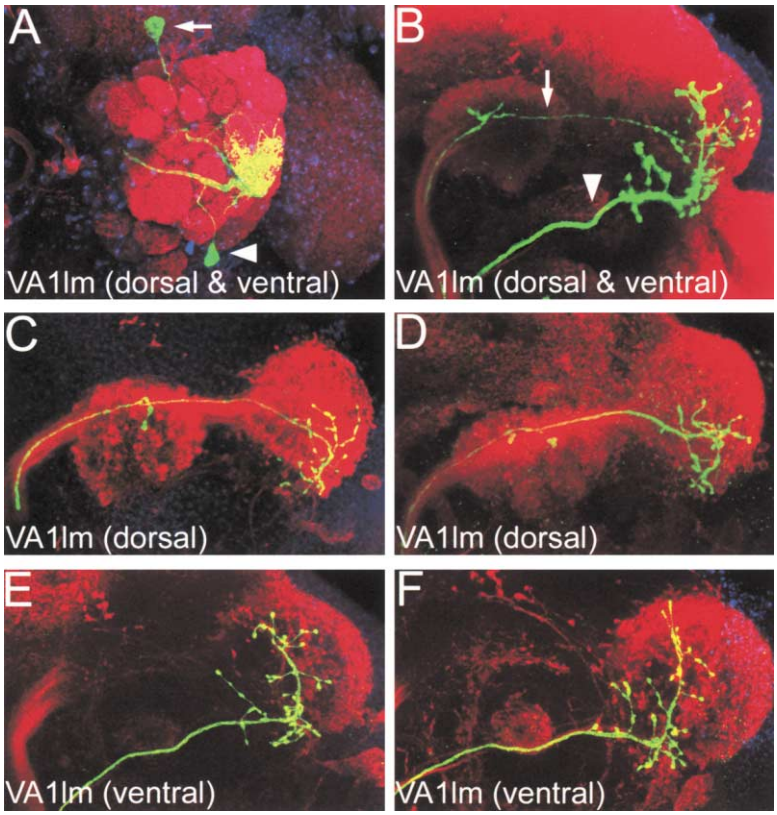

Figure 5. Two Different Classes of PNs Connect the VA1lm Glomerulus to the Protocerebrum

(A) *GH146-Gal4* flies bearing *Hs-flp* and *UAS >CD2,y+ >CD8-GFP* were exposed to a mild heat shock and in rare instances, two PNs that connect to the same glomeruli were labeled. One VA1lm cell body resides within the dorsal group of PNs, and a second within the ventral population. In other experiments with single PNs, individual cells are observed connecting to these two cell groups whose dendrites terminate in the VA1lm glomerulus.

(B) The ventral PNs from VA1lm project via the mACT to the protocerebrum but bypass the mushroom body (arrow). The dorsal VA1lm PN projects via the iACT and branches extensively in the calyx of the mushroom body (arrowhead). The two neurons exhibit distinct projection patterns, which show regions of interdigitation in the lateral aspect of the protocerebrum.

(C–F) Axonal projections from single labeled VA1lm PNs from the dorsal (C and D) and ventral (E and F) population of cell bodies.

and reveal patterns of projection in the protocerebrum that are strikingly similar and almost overlapping. These data demonstrate that each of the multiple neurons innervating a given glomerulus exhibit spatially conserved arborization profiles in the protocerebrum.

Different Projections from the Same Glomerulus

Two glomeruli (VA1lm and DA1) connect to PNs whose cell bodies reside in two different cell groups (Figure 5A). The VA1lm glomerulus is innervated by PNs that reside in the dorsal-anterior group. These dorsal PNs project axons through the iACT, branch to the calyx of the mushroom body, and arborize in a characteristic pattern in the lateral aspect of the protocerebrum (Figures 5B–5D). We have also identified two neurons within the ventral group of PNs that connect to the VA1lm glomerulus. These neurons extend axons through the mACT, bypass the mushroom body, and arborize in the protocerebrum at a location distinct from the termini of the dorsal group of VA1lm neurons (Figures 5B, 5E, and 5F). Thus, PNs that connect to the same glomerulus but maintain their cell bodies in different locations surrounding the antennal lobe exhibit distinct patterns of projections within the protocerebrum.

Projections to the Mushroom Body

The axonal projections in the mushroom body appear far simpler than the rich arborizations in the protocerebrum (Figures 3 and 4). Axons from the inner antennocerebral tract branch to form from 2 to 11 terminal boutons in the mushroom body. The number of boutons appears constant among PNs that innervate a given glomerulus, suggesting that different PNs have different synaptic representation in the mushroom body. For example, the VA1lm dorsal-anterior PNs have 1 to 3 boutons (2 ± 0.6, $n = 7$), whereas the DL1 PNs have 5 to 9 boutons (6.7 ± 1.3, $n = 7$) in the mushroom body (Figures 4E, 4F, 5C, 5D and 6B). In experiments in which single PNs express the fusion protein, synaptobrevin-GFP, a reporter that labels the presynaptic density, the bouton structure is much more prominent in the mushroom body than in the protocerebrum (data not shown). It has been difficult to detect conserved spatial features among like axons in the mushroom body. This may reflect our inability to discern patterns due to inadequate detail, minimizing differences between different PNs. Alternatively, a precise spatial map in the antennal lobe may not be conserved in the mushroom body.

Quantitative Cluster Analysis of Projection Patterns

Visual inspection reveals that projection neurons innervating the same glomerulus exhibit extremely similar patterns of axonal arborization in the protocerebrum. We have performed cluster analysis on 36 PNs that innervate six different glomeruli to provide a more quantitative assessment of the morphologic variation in projection patterns. Cluster analysis of morphologic variables, coupled with principal component analysis (PCA), has been successfully applied to the analysis of stereotypic microcircuitry of the mammalian cortex (Kozloski et al., 2001). We have adapted this procedure to analyze the variation of projection patterns. Confocal image stacks of single-projection neurons were traced and recon-

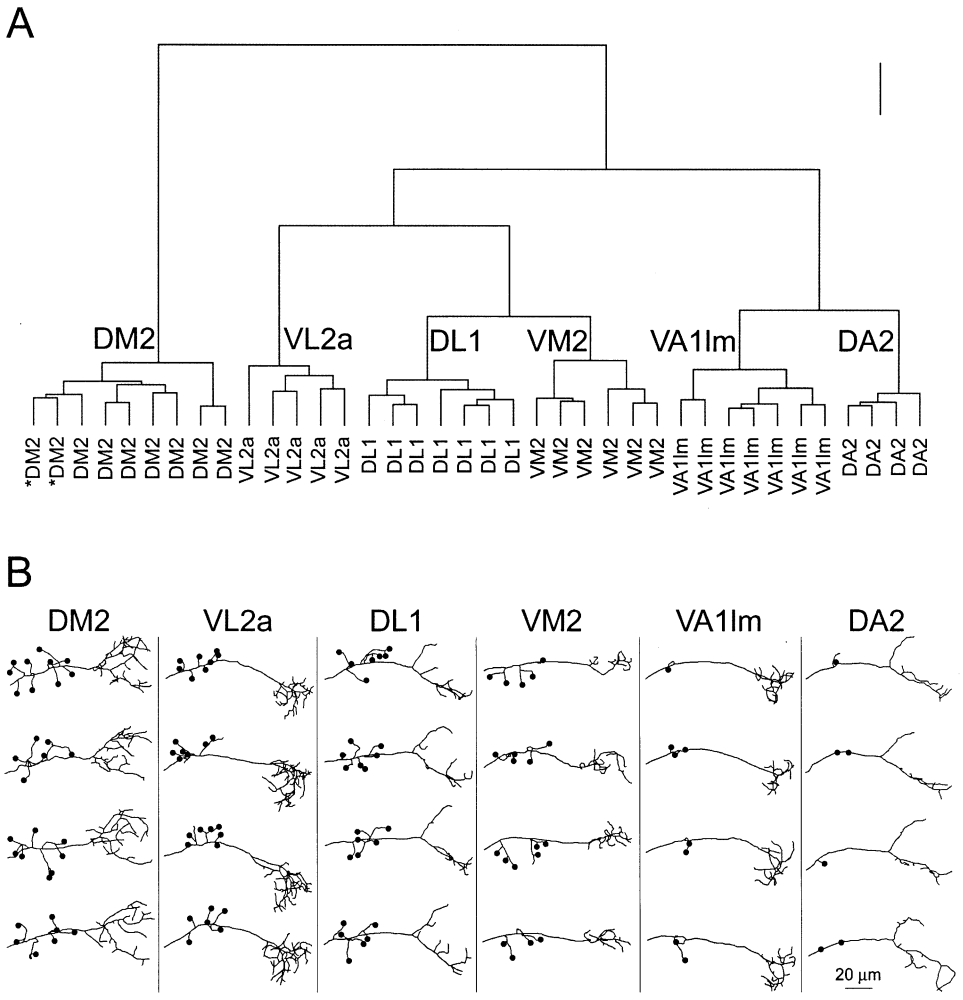

Figure 6. Cluster Analysis of Projection Patterns

(A) A vertical hierarchical tree groups the 38 PNs in 6 different clusters according to their similarity in projection patterns. These six clusters coincide with the six different glomeruli innervated by these 38 PNs. The linkage calculation is based on Euclidian distance. Ward's method was employed for the linkage rule. The vertical bar indicates 5 units in Euclidian distance. The asterisk denotes samples from organisms with surgical removal of the antennae and the maxillary palps. See Experimental Procedures for details.

(B) Camera Lucida patterns of PNs from the six different glomeruli. Twenty-four of the 36 wild-type normal samples in the hierarchical tree are shown. Twelve of the samples have two major branches, a dorsal and a ventral branch in the protocerebrum; the other 12 samples have only the ventral branch. Boutons in the mushroom body calyx are highlighted with filled circles.

structed with vectors to represent axonal branches in three dimensions (Figure 6B). Morphometric parameters, such as branching angle, positional coordinates, and length are measured for each of the branches. PCA, a data reduction method, was then employed to examine 21 parameters describing the axonal arbors, and 17 that were found to make significant contributions to the data set were then subjected to cluster analysis (see Experimental Procedures). This analysis reveals that the 36 different PNs examined cluster into six different groups. These six groups coincide with the six different glomeruli analyzed in this data set (Figure 6A).

The linkage distance measured in Euclidean space represents the dissimilarity between any two PNs calculated from the 17 chosen variables. Thus, the linkage distance between any two dorsal PNs from the VA1lm glomerulus is 3.0 $\pm$ 0.8 and 2.5 $\pm$ 0.4 for any two PNs from the DA2 glomerulus. In contrast, the linkage distance between a VA1lm dorsal PN and any DA2 PN is 4.5 $\pm$ 0.7 (Figure 6), which is significantly different from the values observed within the glomerular classes ($p < 0.001$). These quantitative data provide support for conclusions that derive from visual inspection of projection patterns and confirm that PNs that innervate the same glomerulus share strikingly similar patterns of axonal arborization.

Sensory Input Is Not Required to Maintain a PN Map in the Antennal Lobe and Protocerebrum

We next asked whether olfactory sensory input is required for the maintenance of either the PN dendritic map in the antennal lobe or the PN axonal map in the protocerebrum. Removal of both the antennae and maxillary palps eliminates all olfactory sensory input and results in the rapid degradation of the distal axonal stump in the antennal lobe (Stocker et al., 1990; Gao et al., 2000; Vosshall et al., 2000). The patterns of dendritic and axonal projections were analyzed for 20 individual

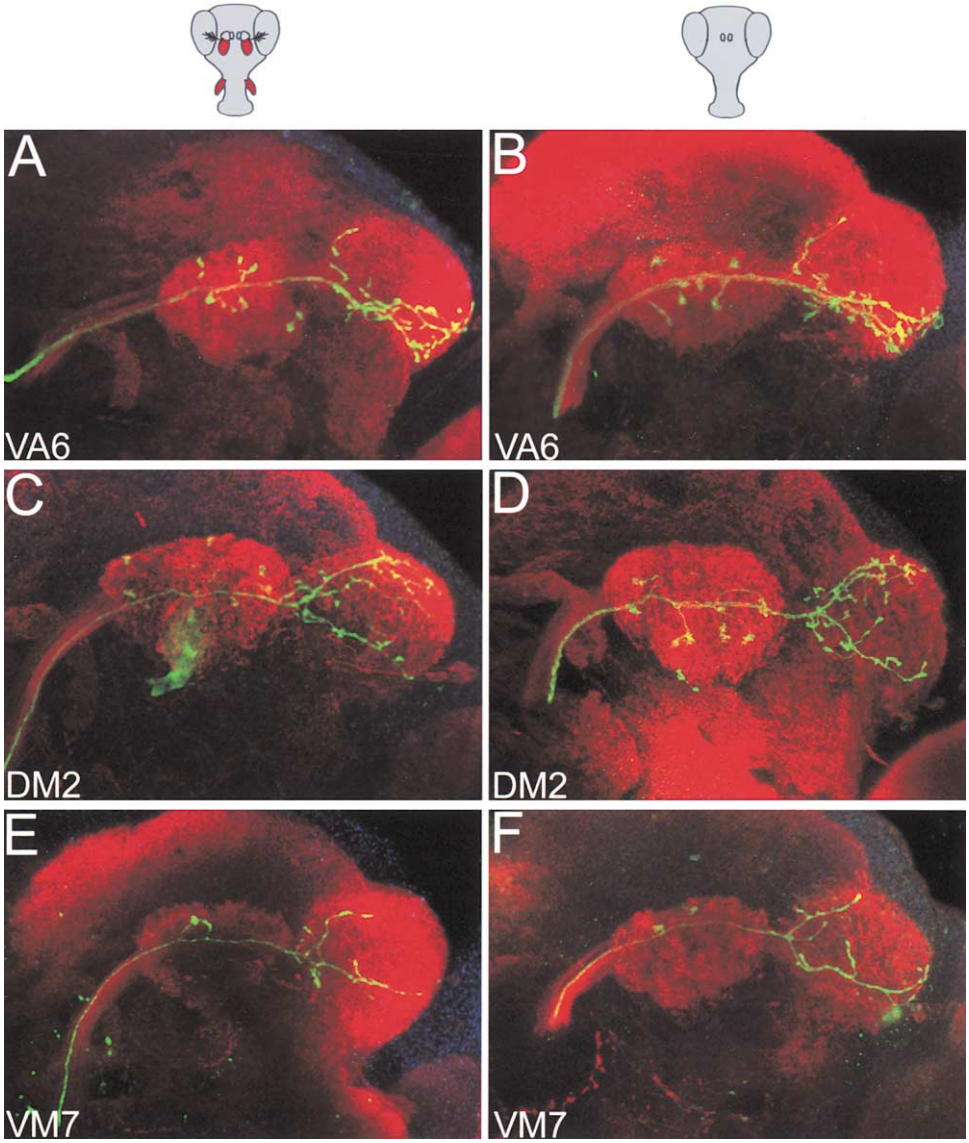

Figure 7. PN Projection Patterns Do Not Change upon Deafferentation

GH146-Gal4 flies, also bearing the transgenes *Hs-flp* and *UAS >CD2,y^{+}>CD8-GFP*, were subjected to mild heat shock during the late larval stage. Antennae and maxillary palps were removed immediately after eclosion. The projection patterns of flies were then examined after 10 days to determine the consequence of the deprivation of olfaction sensory input on the dendritic and axonal projections. Comparison of the projection patterns between wild-type and the deafferented flies for PNs that project to three representative glomeruli, VA6 (A and B), DM2 (C and D), and VM7 (E and F) reveals patterns that are indistinguishable from normal.

projection neurons after surgical removal of all four peripheral olfactory organs at eclosion. Despite the elimination of sensory input, precise dendritic and axonal maps that are indistinguishable from those observed in wild-type flies are observed (Figure 7). These conclusions from visual inspection of projection patterns were confirmed by cluster analysis (Figure 6A). These studies suggest that the precise connectivity between individual glomeruli and defined regions of protocerebrum are maintained after sensory input is eliminated.

Discussion

The organization and functional logic of the peripheral olfactory system appears remarkably similar in fruit flies and mammals. Olfactory sensory neurons in both fly and mouse express only a single receptor from large gene families (Chess et al., 1994; Malnic et al., 1999; Vosshall et al., 2000). Neurons expressing a given receptor project with precision to one or rarely two spatially invariant glomeruli (Ressler et al., 1994; Vassar et al., 1994; Mombaerts et al., 1996; Gao et al., 2000; Vosshall et al., 2000). The convergence of like axons into discrete, insular, glomerular structures provides a two-dimensional map of receptor activation in the first relay station for olfactory information in the brain. In accord with this physical map, functional imaging in both insects and vertebrates reveals that different odors elicit defined spatial patterns of glomerular activation (Friedrich and Korsching, 1997; Joerges et al., 1997; Galizia et al., 1999;

Rubin and Katz, 1999). These data suggest a mechanism of odor discrimination that has been shared, despite the five hundred million years of evolution separating insects from mammals. An odorant will interact with multiple receptors resulting in the activation of a topographically invariant combinatorial of glomeruli. The quality of an odorant may therefore be reflected by defined spatial patterns of activity, first in the antennal lobe (or olfactory bulb), and ultimately in higher olfactory centers in the brain.

In this study, we ask how the precise topographic map in the *Drosophila* antennal lobe is represented in the protocerebrum. We have randomly labeled individual projection neurons using an enhancer trap line that labels a large population of PNs, along with the FLP-out technique that drives the expression of a second reporter in a single neuron. Genetic approaches to visualize individual neurons derive conceptually from the Golgi chrome silver impregnation, "reazione nera," that randomly labels only 1% of the neurons in a particular brain region. This approach, most elegantly employed by Cajal to formulate the neuron theory, permitted the visualization of individual cells along with their processes and provided a first glimpse of specific neural connectivity (Cajal, 1889). The distinction between the genetic approaches (Lee and Luo, 1999) and the histologic experiments of Golgi and Cajal one hundred years earlier is the ability to use genetic markers to more precisely identify partners in the neural circuit.

We observe that the vast majority of PNs send dendrites to only one glomerulus. Projection neurons that innervate the same glomerulus reveal strikingly similar axonal topography, whereas PNs from different glomeruli exhibit very different patterns of projections in the protocerebrum. Thus, neurons that innervate a given glomerulus reveal strikingly stereotyped patterns of axon arborization that are readily apparent upon visual inspection and are confirmed by more quantitative cluster analysis. These conclusions derive from analysis of less than half of the total number of PNs, and additional analysis will be required to determine whether they can be extended to the complete set.

An interesting variation of this pattern is observed for at least two glomeruli, VA1lm and DA1. PNs that receive input from these glomeruli have cell bodies that reside within two distinct cell groups surrounding the antennal lobe. PNs that connect with VA1lm, for example, reside in both the dorsal and ventral cell groups. The ventral PNs bypass the mushroom body and project to the anterior-medial aspect of the protocerebrum, whereas the dorsal PNs branch to the MB and arborize in more lateral positions of the protocerebrum. These invariant parallel projections can therefore deliver similar information to different parts of the fly brain.

The projections of second-order olfactory neurons have been analyzed previously in other insects by dye injection (Burrows et al., 1982; Homberg, 1984; Homberg et al., 1988), but in most instances it has not been possible to reproducibly distinguish the different PNs. In the moth, dye injections reveal that neurons from the sexually dimorphic macroglomerular complex exhibit projection patterns different from the major class of PNs (Homberg et al., 1988). Our data examine the projections of identified neurons and reveal a striking invariance in the spatial patterns of axon arbors from PNs that innervate a given glomerulus. The stereotypy of neurons and their connections is characteristic of invertebrate nervous systems (see, for example, Ward et al., 1975; Bentley and Keshishian, 1982; Raper et al., 1983; Johansen et al., 1989) and may be a prominent feature of the vertebrate brain (Kozloski et al., 2001). The inordinate precision of connections is likely to reflect a high degree of innate specification of individual neurons that will ultimately dictate the path and character of its projections. This must be complemented by precise guidance information along a neuron's path that governs the position and character of its arbors. The end result is a pattern of apparently precise connectivity that assures the specificity of information transfer.

The precision of projections of PNs reveals a spatial representation of glomerular activity in higher brain centers, but the character of the map differs from that observed in the antennal lobe. Axon arbors in the protocerebrum are diffuse and extensive, often extending the entire dorsal-ventral dimension of the brain hemisphere. This is in sharp contrast to the tight convergence of primary sensory axons whose arbors are often restricted to small 5–10 μm spherical glomeruli. As a consequence, the projections from different glomeruli, although spatially distinct, often interdigitate. Thus, the "point-to-point" segregation observed in the antennal lobe is "degraded" in the second-order projections to the protocerebrum. This affords an opportunity for the convergence of inputs from multiple different glomeruli essential for higher order processing. Third-order neurons in the protocerebrum might synapse on PNs from multiple distinct glomeruli, a necessary step in decoding spatial patterns to allow the discrimination of odor and behavioral responses.

Similar conclusions emerge from recent experiments that employ genetically encoded transneuronal tracers in the mouse olfactory system (Zou et al., 2001). Mitral cells that receive input from a single glomerulus project to defined regions of the piriform cortex that are more extensive than the glomerular segregation. Moreover, overlap in the projection patterns of different glomeruli affords the opportunity for integration of olfactory information at these higher olfactory centers.

Odor-Evoked Activity and the Maintenance of a Topographic Map

In both mice and flies, olfactory sensory neurons expressing a given odorant receptor project with precision to spatially invariant glomeruli within the olfactory bulb or antennal lobe (Gao et al., 2000; Vosshall et al., 2000; Scott et al., 2001). In *Drosophila*, an invariant spatial representation is also observed for projection neurons that connect a given glomerulus with the protocerebrum. These observations raise the question as to how the maps of primary and secondary sensory projections are established and maintained. In one model, spatially restricted guidance cues may be the sole determinants specifying an invariant pattern of connections during development. Other models invoke activity-dependent processes that may operate either alone or in concert with target-derived guidance cues to achieve the precision of connections observed both in the antennal lobe and protocerebrum.

In mice, odor-evoked activity is not required to either generate or maintain a topographic map of sensory projections in the olfactory bulb (Belluscio et al., 1998; Lin et al., 2000; Zheng et al., 2000). Only subtle alterations in glomerular targeting are associated with mutants deficient in sensory input. Preliminary observations in the fly similarly suggest that olfactory experience is not required to generate a map in the antennal lobe since primary sensory axons arrive at specific glomeruli prior to receptor expression (Clyne et al., 1999; Jhaveri et al., 2000; Fishilevich and Vosshall, personal communication). These data suggest that the establishment of precise connections of sensory neurons in the antennal lobe is likely to require positional cues that guide axons without a contribution from olfactory experience. Moreover, the precision of the map in the antennal lobe in which sensory neurons bearing a given odorant receptor and a small defined set of PNs project to a single glomerulus suggest that common cues may guide both primary sensory axons and PN dendrites to a common glomerular target.

In this study, we demonstrate that removal of the peripheral olfactory organs does not perturb the second order map of projections from the antennal lobe to the protocerebrum. In *Drosophila*, therefore, olfactory input is not likely to be required for the maintenance of either primary or secondary sensory maps. A more complex scenario is emerging from the analysis of the role of activity in the development and maintenance of higher order projections in the visual system. Ocular dominance and orientation columns develop in the mammalian cortex in the absence of visual input (Crair et al., 1998; Crowley and Katz, 1999, 2000). Different patterns of sensory activity, however, can have profoundly different effects on the maturation of orientation selectivity (White et al., 2001). Moreover, the maintenance of orientation selectivity of cortical neurons requires subsequent visual experience since these maps degrade with sensory deprivation during the critical period (Crair et al., 1998). The concept of the critical period in the mammalian visual system during which visual input shapes connectivity does not appear to have an analogous counterpart in the olfactory system of either flies or mammals.

Implications for Sensory Processing

Different odorants elicit spatially defined patterns of glomerular activity in the antennal lobe. The antennal lobe therefore provides a two-dimensional map that identifies which of the numerous receptors have been activated within the antenna. The quality of an olfactory stimulus could therefore be encoded by the specific combination of glomeruli activated by a given odorant. This model of olfactory perception shares several basic features with perception in other sensory systems. For example, the brain analyzes a visual image by interpreting the individual components of the image: form, location, movement, and color (Livingstone and Hubel, 1987; Zeki and Shipp, 1988). The unity of a visual image is accomplished by several parallel processing pathways, such that the image is initially dissected into tractable components and then reconstructed in higher visual centers in the cortex. A similar logic may be employed to discriminate olfactory stimuli. Olfactory processing will initially require that the structural elements of an odor activate a unique subset of receptors, which in turn results in the activation of a unique subset of glomeruli. The odorous stimulus must then be reconstructed in higher sensory centers which determine which of the numerous glomeruli have been activated.

How are the individual components that represent sensory image bound into a coherent whole? One model postulates the convergence of information from deconstructed patterns in the antennal lobe to "cardinal cell assemblies" that sit at the top of a hierarchical perceptual system in higher brain areas. The identification of a spatially invariant sensory map in the fly protocerebrum that is divergent and no longer exhibits the insular segregation of like axons observed in the antennal lobe affords an opportunity for integration from multiple glomerular inputs by such cardinal cells. Hence, the notion of grandmother cells in vision (Barlow, 1972) and jasmine cells in olfaction. An alternative hypothesis postulates that a given odor is defined by a temporal code of neural elements (Laurent, 1999). In this model, oscillations, phasing, and synchrony are more relevant attributes of neural identity and odor quality than position. Although considerable evidence has been provided for the coordination of spike timing, the question as to whether synchrony and phasing serve an informational role in cortical processing remains unresolved. Whatever the mechanism, the persistence of an invariant topographic map reflecting receptor activation in the periphery in higher brain centers is likely to contribute to the interpretation and discrimination of olfactory information.

Experimental Procedures

Experimental Animals and Transgenes

Flies were raised on standard medium at 25°C. To reduce background fluorescence, flies aged less than 3 days were used for all experiments unless otherwise indicated. The following transgenic lines were used in a combination of the UAS/Gal4 (Brand and Perrimon, 1993) and the FLP-out (Basler and Struhl, 1994) techniques to generate samples containing single PNs:

GH146-Gal4 (Stocker et al., 1997); *UAS >CD2, y$^+$ >CD8-GFP*, kindly provided by Gary Struhl; *UAS-GFPnls* (Struhl and Greenwald, 2001; *GFPnls* encodes a nuclear-localized form of the GFP molecule); and *Hs-flp* (Basler and Struhl, 1994).

Larvae containing three transgenes, *UAS >CD2,y$^+$ >CD8-GFP*, *Hs-flp*, and *GH146-Gal4*, were given a mild heat shock (32°C for 1 hr) at late third instar to remove the FLP-out cassette *CD2,y$^+$* in a subset of the neurons. At room temperature (25°C), samples containing single GFP-labeled PNs were also observed without receiving a heat shock, probably due to a leaky expression of *Hs-flp*. Thus, some samples were generated without heat shock.

Peripheral deafferentation was performed by removing both antennae and maxillary palps from anesthetized, newly eclosed flies with forceps. Animals were allowed to recover in fresh vials and aged for 10 days at 25°C before projection patterns were analyzed.

Immunocytochemistry and Confocal Microscopy

Fly heads were fixed in PB containing 4% paraformaldehyde and 0.1% Triton X-100 for 3 hr on ice and subsequently rinsed with PBST (0.1% Triton X-100 in PBS) three times. Microdissection was performed in PBST to remove the cuticle and connective tissues. Samples were incubated in heat-inactivated goat antiserum for 2 hr, then in a cocktail of primary antibodies including a mouse monoclonal nc82 (dilution of 1:20), Serotech mouse anti-CD2 (1:1000), and Molecular Probes rabbit anti-GFP (1:1000) overnight. Samples were washed three times for 10 min with PBST before incubation

for 2 hr with a cocktail of secondary antibodies, which include goat anti-mouse conjugated with Alexa Fluor 568 (1:1000), goat anti-rabbit conjugated with Alexa Fluor 488 (1:1000), and a 1:1000 dilution of TOTO-3 (Molecular Probes). After three 10 min rinses with PBST, brains were mounted in Vectashield (Vector Labs) using small #1 thickness coverslips as spacers. Image stacks were taken with a Biorad 1024 confocal microscope. A stack of confocal images at 1–2 μm step was collected for each PN in the calyx-protocerebrum region, and another stack of images was collected for the antennal lobe region with a Nikon 60$\times$ objective lens. Glomeruli were identified and named using the antennal lobe map established by Laissue et al. (1999). We examined approximately 2000 brains and have obtained over 200 brains labeled with single PNs.

Cluster Analysis of Projection Patterns

PNs innervating the glomeruli VL2a, VA1lm, VM2, DM2, DL1, and DA2 were selected for quantitative morphological analysis because their patterns of axonal arbors in the mushroom body and the protocerebrum are representative in degree of complexity. Confocal image stacks were traced and reconstructed with Neurolucida (Version 4.33, MicroBrightField, Colchester, VT). The axonal projection pattern of PNs was the focus of this analysis; therefore, dendritic arborization in the antennal lobe and the cell body were not included in this analysis. Thus, tracing of each PN started at the mushroom body. At the entry point of the lateral protocerebrum, some PNs separate into dorsal and ventral branches, whereas other PNs have a ventral but no dorsal branch. Twenty-one morphological parameters describing branching pattern in three regions, calyx of the mushroom body, dorsal branch, and the ventral branch in the protocerebrum, were measured from the reconstructed neurons with NeuroExplorer (Version 3.30, MicroBrightField, Colchester, VT). These 21 parameters are: End_d, number of termini in the dorsal branch; L_d, total length of the dorsal branch; BrO_d, highest order of the dorsal branch; End_v, number of termini in the ventral branch; L_v, total length of the ventral branch; Maj_L_v, main axon length from the entry point of the protocerebrum to the distal terminus of the ventral branch; Ratio_v, (1- Maj_L_v/L_v); P_Ang_v, planer angle between the ventral branch and the branch it branches from; XY_Ang_v, angle in the XY plan between the ventral branch and the branch it branches from; Z_Ang_v, angle in the XZ plan between the ventral branch and the branch it branches from; Abs_X_v, lateral centroid coordinate of the terminal polygon of the ventral branch in reference to the protocerebrum entry point; Y_v, dorsoventral centroid coordinate of the terminal polygon of the ventral branch in reference to the protocerebrum entry point; Z_v, anteroposterior centroid coordinate of the terminal polygon of the ventral branch in reference to the protocerebrum entry point; D_v, distance of the terminal polygon centroid to the protocerebrum entry point; BrO_v, highest order of the ventral branch; D1N_v, distance from the protocerebrum entry point to the first node in the ventral branch; End_c, number of termini in the calyx region; L_Br_v, length of higher order branch in the calyx region; L_c, total neurite length in the calyx region; Ratio_c, L_Br_v/ L_c; and Var_c, number of boutons in the calyx region. nSyb-GFP, a fusion protein between neuronal synaptobrevin and GFP (Estes et al., 2000), was very localized to boutons in the mushroom body calyx but more distributed along axons in the protocerebrum region (A.M.W., J.W.W., and R.A., unpublished data). Therefore, the number of boutons was counted only in the calyx.

Principal component analysis (PCA) was utilized to identify the parameters that make major contributions to the group variance. For the 36 PNs and 21 variables, 7 independent factors with an eigen value larger than 0.7 were identified and accounted for $>$90% of the total variance. Seventeen (except Maj_L_v, P_Ang_v, Abs_X_v, and D_v) of the aforementioned 21 variables, in varimax factor rotation, made significant contributions (loading factor $>$0.7) to the 7 independent factors and were therefore selected for subsequent cluster analysis (CA). For all the variables, standardization was performed before analysis to ensure equal weight for each variable. PCA and CA were performed with Statistica for Window (Version 6.0, StatSoft, Tulsa, OK). CA was performed with Ward's method, which seeks clusters that produce the smallest possible increase in the error sum of squares. The linkage was measured in Euclidian distance.

PCA, however, does not provide information about the minimum set of morphometrical variables to separate these different patterns. We then sequentially eliminated one variable at a time and kept those variables that maximize the differences between clusters. We discovered that these six patterns can be fully separated by using only four variables, L_d, Ratio_v, Y_v, and Var_c. Essentially, one variable describing the axon length of the dorsal branch, two variables for the ventral branch, and one variable for the number of boutons in the mushroom body. All numbers are presented as average $\pm$ standard deviation unless otherwise indicated.

Acknowledgments

We thank Gary Struhl for kindly providing *UAS >CD2,y$^+$ >*CD8-GFP, *Hs-flp*, and *UAS-GFPnls* transgenic lines and for continual advice in the performance of these experiments. In addition, we thank Reinhard Stocker for providing the *GH146-Gal4* line and the nc82 monoclonal antibody; Rafa Yuste, Areti Tsiola, and Farid Hamzei-Sichani for help with the cluster analysis; and Phyllis Kisloff for assistance in preparing the manuscript. We also thank Liqun Luo and the members of his laboratory for open communication of data during the course of these studies. We thank Tom Jessell, Gary Struhl, Andrew Tomlinson, Leslie Vosshall, Rafa Yuste, and members of the Axel Lab for critical comments on the manuscript. This research was supported by the Howard Hughes Medical Institute (R.A.) and by a grant from the National Institutes of Health (NIMH) MH50733 (R.A., J.W.W., and A.M.W.).

Received: December 18, 2001
Revised: March 4, 2002

References

Barlow, H.B. (1972). Single units and sensation: a neuron doctrine for perceptual psychology? Perception *1*, 371–394.

Basler, K., and Struhl, G. (1994). Compartment boundaries and the control of *Drosophila* limb pattern by hedgehog protein. Nature *368*, 208–214.

Belluscio, L., Gold, G.H., Nemes, A., and Axel, R. (1998). Mice deficient in G(olf) are anosmic. Neuron *20*, 69–81.

Bentley, D., and Keshishian, H. (1982). Pathfinding by peripheral pioneer neurons in grasshoppers. Science *218*, 1082–1088.

Brand, A.H., and Perrimon, N. (1993). Targeted gene expression as a means of altering cell fates and generating dominant phenotypes. Development *118*, 401–415.

Burrows, M., Boeckh, J., and Esslen, J. (1982). Physiological and morphological properties of interneurones in the deutocerebrum of male cockroaches which respond to female pheromone. J Comp Physiol. *145*, 447–457.

Cajal, S.R. (1889). Manual de Histologia normal y Tecnica micrografica. (Valencia: P. Aguilar).

Chess, A., Simon, I., Cedar, H., and Axel, R. (1994). Allelic inactivation regulates olfactory receptor gene expression. Cell *78*, 823–834.

Clyne, P.J., Warr, C.G., Freeman, M.R., Lessing, D., Kim, J., and Carlson, J.R. (1999). A novel family of divergent seven-transmembrane proteins: candidate odorant receptors in *Drosophila*. Neuron *22*, 327–338.

Crair, M.C., Gillespie, D.C., and Stryker, M.P. (1998). The role of visual experience in the development of columns in cat visual cortex. Science *279*, 566–570.

Crowley, J.C., and Katz, L.C. (1999). Development of ocular dominance columns in the absence of retinal input. Nat. Neurosci. *2*, 1125–1130.

Crowley, J.C., and Katz, L.C. (2000). Early development of ocular dominance columns. Science *290*, 1321–1324.

Dunipace, L., Meister, S., McNealy, C., and Amrein, H. (2001). Spatially restricted expression of candidate taste receptors in the *Drosophila* gustatory system. Curr. Biol. *11*, 822–835.

Estes, P.E., Ho, G., Narayanan, R., and Ramaswami, M. (2000). Synaptic localization and restricted diffusion of a *Drosophila* neuronal

synaptobrevin-green fluorescent protein chimera in vivo. J. Neurogenet. *13*, 233–255.

Friedrich, R.W., and Korsching, S.I. (1997). Combinatorial and chemotopic odorant coding in the zebrafish olfactory bulb visualized by optical imaging. Neuron *18*, 737–752.

Galizia, C.G., Sachse, S., Rappert, A., and Menzel, R. (1999). The glomerular code for odor representation is species specific in the honeybee *Apis mellifera*. Nat. Neurosci. *2*, 473–478.

Gao, Q., and Chess, A. (1999). Identification of candidate *Drosophila* olfactory receptors from genomic DNA sequence. Genomics *60*, 31–39.

Gao, Q., Yuan, B., and Chess, A. (2000). Convergent projections of *Drosophila* olfactory neurons to specific glomeruli in the antennal lobe. Nat. Neurosci. *3*, 780–785.

Homberg, U. (1984). Processing of antennal information in extrinsic mushroom body neurons of the bee brain. J. Comp. Physiol. [A] *154*, 825–836.

Homberg, U., Montague, R.A., and Hildebrand, J.G. (1988). Anatomy of antenno-cerebral pathways in the brain of the sphinx moth *Manduca sexta*. Cell Tissue Res. *254*, 255–281.

Ito, K., Suzuki, K., Estes, P., Ramaswami, M., Yamamoto, D., and Strausfeld, N.J. (1998). The organization of extrinsic neurons and their implications in the functional roles of the mushroom bodies in *Drosophila melanogaster* Meigen. Learn. Mem. *5*, 52–77.

Johansen, J., Halpern, M.E., Johansen, K.M., and Keshishian, H. (1989). Stereotypic morphology of glutamatergic synapses on identified muscle cells of *Drosophila* larvae. J. Neurosci. *9*, 710–725.

Jefferis, G.S.X.E., Marin, E.C., Stocker, R.F., and Luo, L. (2001). Target neuron prespecification in the olfactory map of *Drosophila*. Nature *418*, 204–208.

Jhaveri, D., Sen, A., and Rodrigues, V. (2000). Mechanisms underlying olfactory neuronal connectivity in *Drosophila*—the atonal lineage organizes the periphery while sensory neurons and glia pattern the olfactory lobe. Dev Biol. *226*, 73–87.

Joerges, J., Küttner, A., Galizia, C.G., and Menzel, R. (1997). Representation of odours and odour mixtures visualized in the honeybee brain. Nature *387*, 285–288.

Kozloski, J., Hamzei-Sichani, F., and Yuste, R. (2001). Stereotyped position of local synaptic targets in neocortex. Science *293*, 868–872.

Laissue, P.P., Reiter, C., Hiesinger, P.R., Halter, S., Fischbach, K.F., and Stocker, R.F. (1999). Three-dimensional reconstruction of the antennal lobe in *Drosophila melanogaster*. J. Comp. Neurol. *405*, 543–552.

Laurent, G. (1999). A systems perspective on early olfactory coding. Science *286*, 723–728.

Lee, T., and Luo, L. (1999). Mosaic analysis with a repressible cell marker for studies of gene function in neuronal morphogenesis. Neuron *22*, 451–461.

Lin, D., Wang, F., Lowe, G., Gold, G., Axel, R., Ngai, J., and Brunet, L. (2000). Formation of precise connections in the olfactory bulb occurs in the absence of odorant-evoked neuronal activity. Neuron *26*, 69–80.

Livingstone, M.S., and Hubel, D.H. (1987). Psychophysical evidence for separate channels for the perception of form, color, movement, and depth. J. Neurosci. *7*, 3416–3468.

Malnic, B., Hirono, J., Sato, T., and Buck, L.B. (1999). Combinatorial receptor codes for odors. Cell *96*, 713–723.

Marin, E.C., Jefferis, G.S.X.E., Komiyama, T., Zhu, H., and Luo, L. (2002). Representation of the glomerular olfactory map in the *Drosophila* brain. Cell *109*, this issue, 243–255.

Mombaerts, P., Wang, F., Dulac, C., Chao, S.K., Nemes, A., Mendelsohn, M., Edmondson, J., and Axel, R. (1996). Visualizing an olfactory sensory map. Cell *87*, 675–686.

Nellen, D., Burke, R., Struhl, G., and Basler, K. (1996). Direct and long-range action of a DPP morphogen gradient. Cell *85*, 357–368.

Raper, J.A., Bastiani, M., and Goodman, C.S. (1982). Pathfinding by neuronal growth cones in grasshopper embryos. J. Neurosci. *3*, 20–30.

Raper, J.A., Bastiani, M., and Goodman, C.S. (1983). Pathfinding by neuronal growth cones in grasshopper embryos. I. Divergent choices made by the growth cones of sibling neurons. J. Neurosci. *3*, 20–30.

Ressler, K.J., Sullivan, S.L., and Buck, L.B. (1994). Information coding in the olfactory system: evidence for a stereotyped and highly organized epitope map in the olfactory bulb. Cell *79*, 1245–1255.

Rodrigues, V. (1988). Spatial coding of olfactory information in the antennal lobe of *Drosophila melanogaster*. Brain Res. *453*, 299–307.

Rodrigues, V., and Buchner, E. (1984). [^{3}H]2-deoxyglucose mapping of odor-induced neuronal activity in the antennal lobes of *Drosophila melanogaster*. Brain Res. *324*, 374–378.

Rubin, B.D., and Katz, L.C. (1999). Optical imaging of odorant representations in the mammalian olfactory bulb. Neuron *23*, 499–511.

Scott, K., Brady, R., Jr., Cravchik, A., Morozov, P., Rzhetsky, A., Zuker, C., and Axel, R. (2001). A chemosensory gene family encoding candidate gustatory and olfactory receptors in *Drosophila*. Cell *104*, 661–673.

Stocker, R.F. (1994). The organization of the chemosensory system in *Drosophila melanogaster*: a review. Cell Tissue Res. *275*, 3–26.

Stocker, R.F., Lienhard, M.C., Borst, A., and Fischbach, K.F. (1990). Neuronal architecture of the antennal lobe in *Drosophila melanogaster*. Cell Tissue Res. *262*, 9–34.

Stocker, R.F., Heimbeck, G., Gendre, N., and de Belle, J.S. (1997). Neuroblast ablation in *Drosophila* P[GAL4] lines reveals origins of olfactory interneurons. J. Neurobiol. *32*, 443–456.

Stortkuhl, K.F., and Kettler, R. (2001). Functional analysis of an olfactory receptor in *Drosophila melanogaster*. Proc. Natl. Acad. Sci. USA *98*, 9381–9385.

Struhl, G., and Greenwald, I. (2001). Presenilin-mediated transmembrane cleavage is required for *Notch* signal transduction in *Drosophila*. Proc. Natl. Acad. Sci. USA *98*, 229–234.

Vassar, R., Chao, S.K., Sitcheran, R., Nunez, J.M., Vosshall, L.B., and Axel, R. (1994). Topographic organization of sensory projections to the olfactory bulb. Cell *79*, 981–991.

Vosshall, L.B., Wong, A.M., and Axel, R. (2000). An olfactory sensory map in the fly brain. Cell *102*, 147–159.

Ward, S., Thomson, N., White, J.G., and Brenner, S. (1975). Electron microscopical reconstruction of the anterior sensory anatomy of the nematode *Caenorhabditis elegans*. J. Comp. Neurol. *160*, 313–337.

Wetzel, C.H., Behrendt, H.J., Gisselmann, G., Stortkuhl, K.F., Hoveman, B., and Hatt, H. (2001). Functional expression and characterization of a *Drosophila* odorant receptor in a heterologous cell system. Proc. Natl. Acad. Sci. USA *98*, 9377–9380.

White, L.E., Coppola, D.M., and Fitzpatrick, D. (2001). The contribution of sensory experience to the maturation of orientation selectivity in ferret visual cortex. Nature *411*, 1049–1052.

Zecca, M., Basler, K., and Struhl, G. (1996). Direct and long-range action of a wingless morphogen gradient. Cell *87*, 833–844.

Zeki, S., and Shipp, S. (1988). The functional logic of cortical connections. Nature *335*, 311–317.

Zheng, C., Feinstein, P., Bozza, T., Rodriguez, I., and Mombaerts, P. (2000). Peripheral olfactory projections are differentially affected in mice deficient in a cyclic nucleotide-gated channel subunit. Neuron *26*, 81–91.

Zou, Z., Horowitz, L.F., Montmayeur, J.P., Snapper, S., and Buck, L.B. (2001). Genetic tracing reveals a stereotyped sensory map in the olfactory cortex. Nature *414*, 173–179.